

# **Superconducting Circuits for Quantum Computing and Quantum Sensing**

**Robert McDermott, UW-Madison**

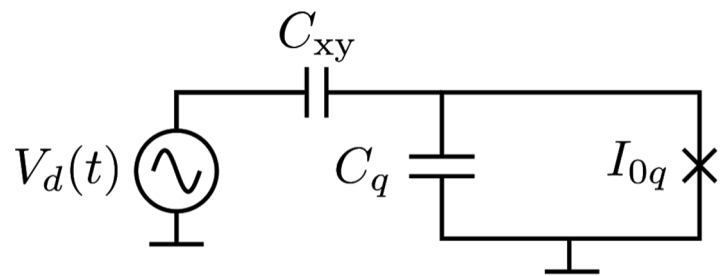
**ICEPP Workshop  
March 9, 2022**



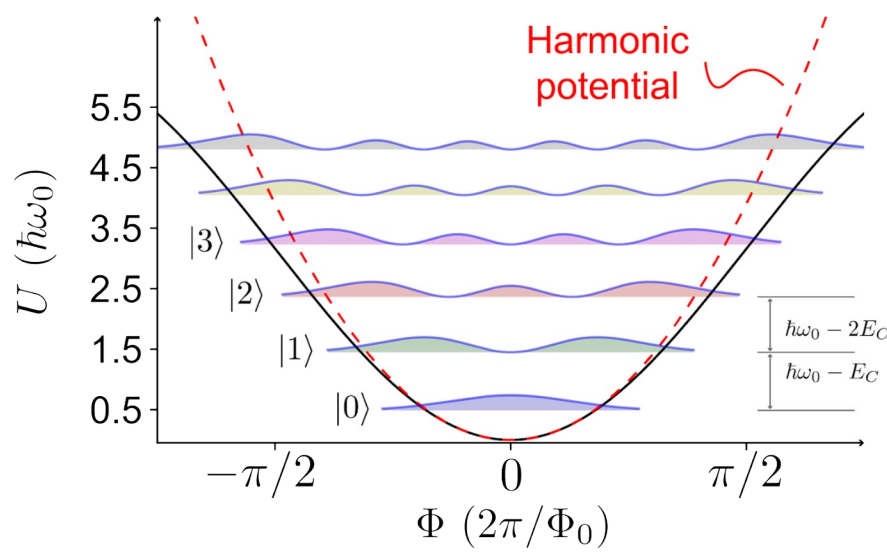
# Outline

- Introduction to SC qubits
- Requirements for fault tolerance
- Correlated errors from particle impacts; mitigation
- Photon-assisted QP poisoning
- Qubit-based sensors for dark matter detection

# Transmon qubit



$$\hat{H} = \frac{\hat{Q}^2}{2C_\Sigma} - E_J \cos\left(\frac{2\pi\Phi}{\Phi_0}\right)$$

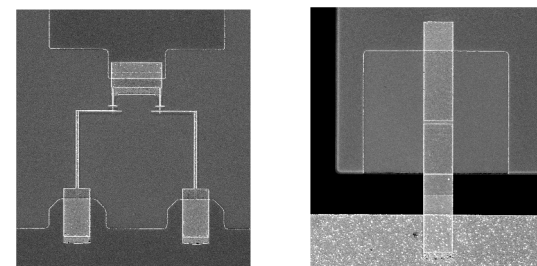
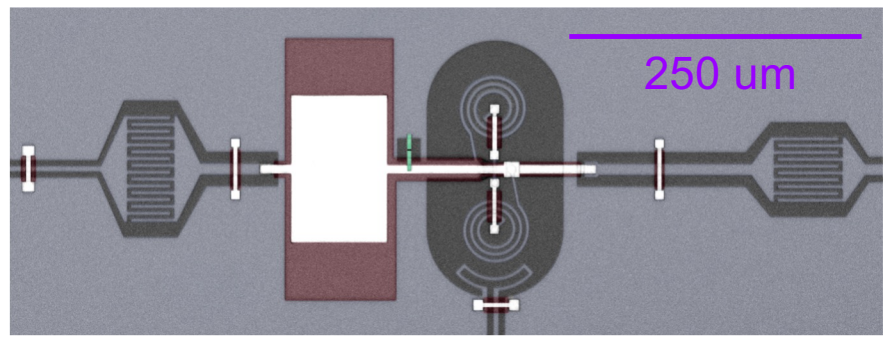
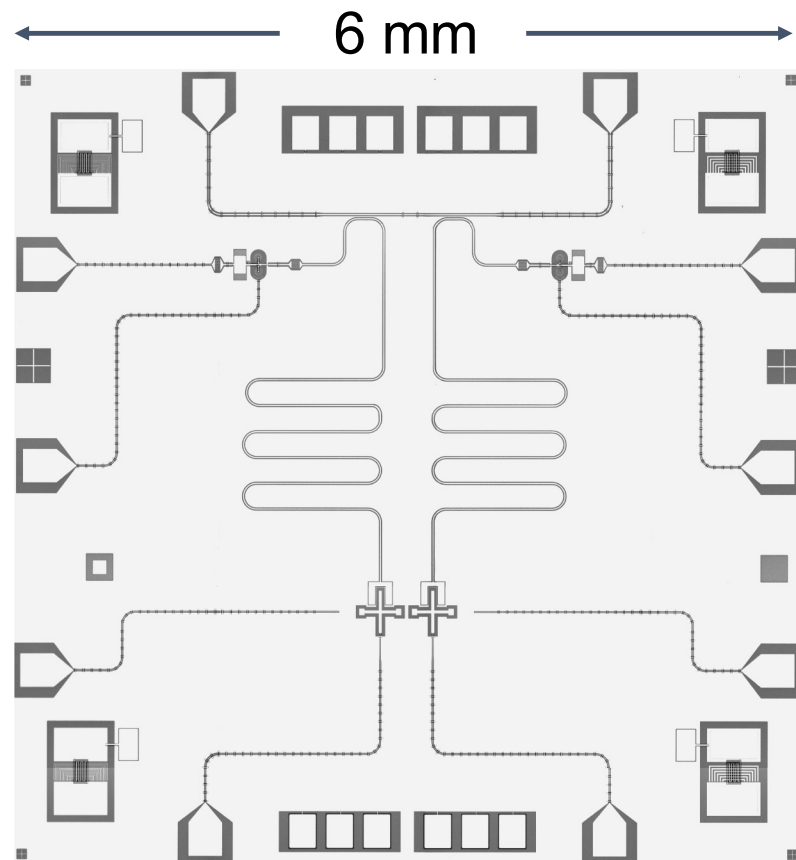


$$E_J = I_{0q}\Phi_0/2\pi$$

$$E_C = e^2/2C_\Sigma$$

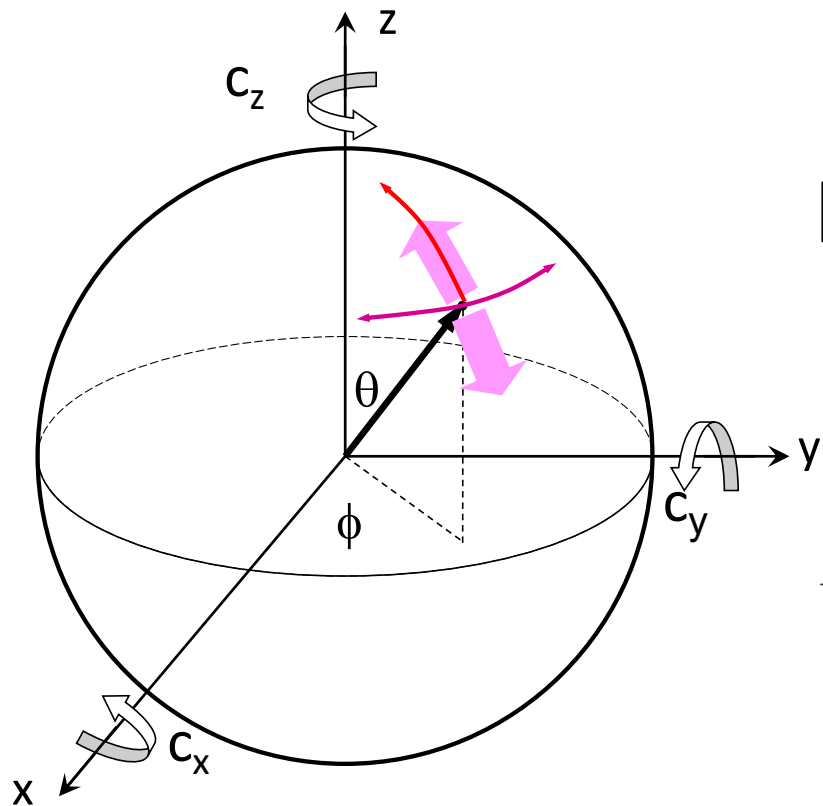
$$\omega_0 = \sqrt{8E_J E_C}/\hbar$$

# Chip layout



Opremcak *et al.*, PRX 11, 011027 (2021)

# Bloch sphere representation

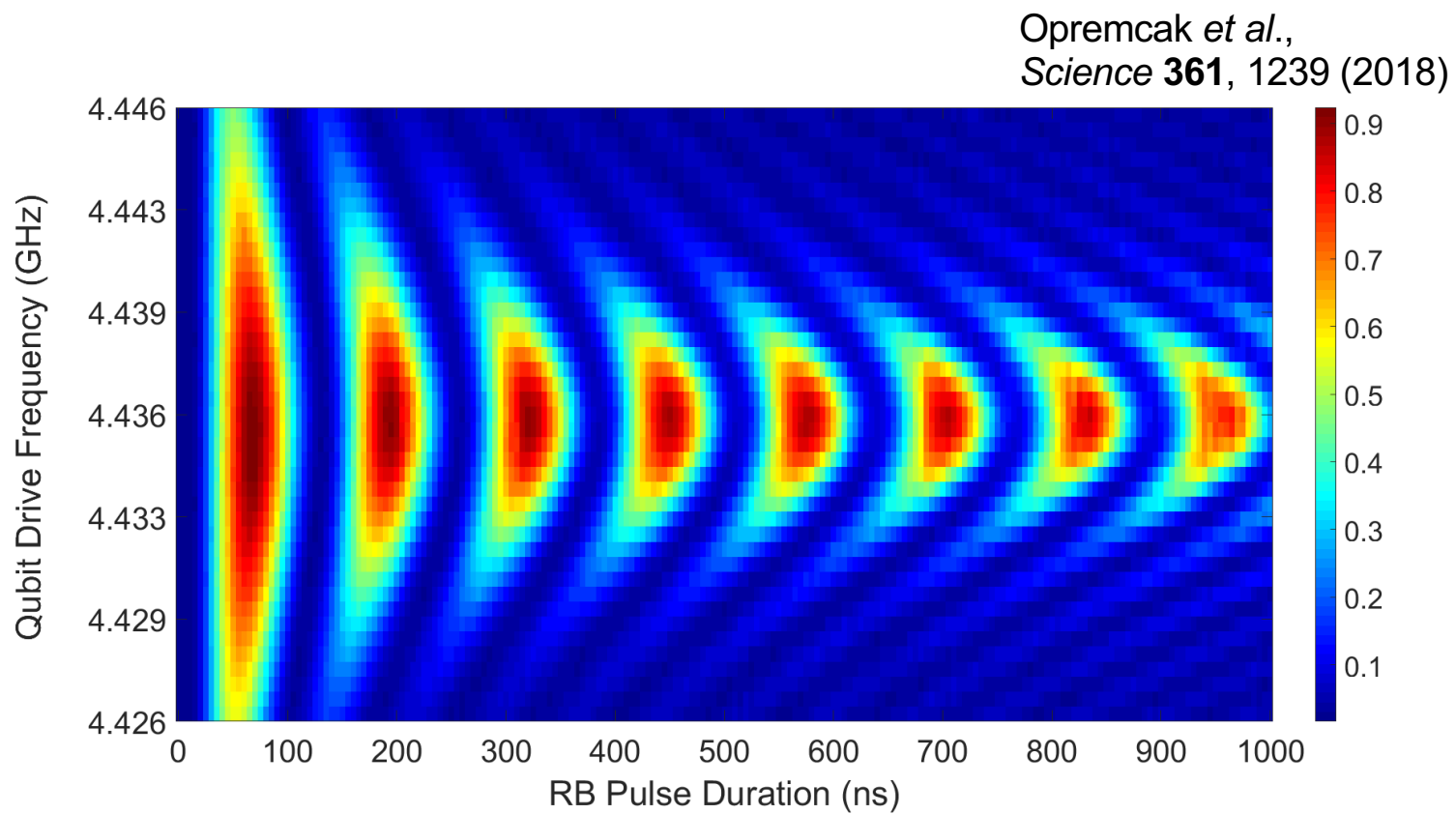


$$|\Psi\rangle = \cos \frac{\theta}{2} |0\rangle + e^{i\phi} \sin \frac{\theta}{2} |1\rangle$$

$$\hat{H} = \frac{\hat{Q}^2}{2C_\Sigma} - E_J \cos\left(\frac{2\pi\hat{\Phi}}{\Phi_0}\right) + \frac{C_{xy}}{C_\Sigma} V_d(t) \hat{Q}$$

controlled dynamically

# Qubit Rabi oscillations



# Towards fault-tolerant QC

The challenge:

- Pauli X and Z don't commute  
(impossible to  
simultaneously monitor  
bit and phase flips  
using naïve approach)

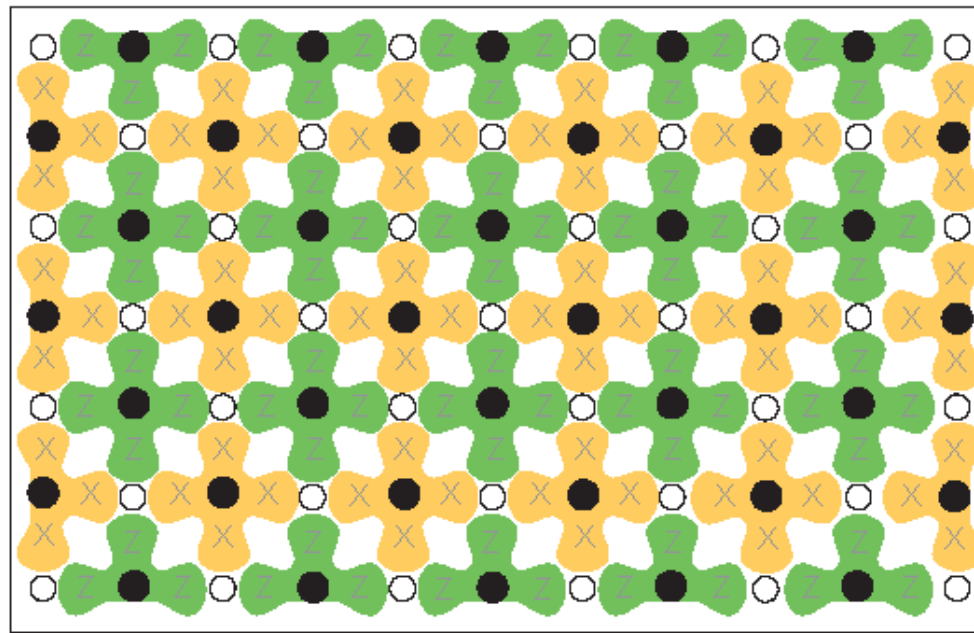
However:

- Multiqubit parity operators (e.g., XXXX, ZZZZ) do commute!  
possible in principle to uniquely identify errors in multiqubit arrays

# Towards fault-tolerant QC

Two-dimensional  
surface code

Fowler et al.,  
PRA 86, 032324  
(2012)



single QB gates: 99.9%  
entangling gates: 99%  
measurement: 90%

(generally target one order  
of magnitude lower infidelity)

Assumption: NO correlated errors

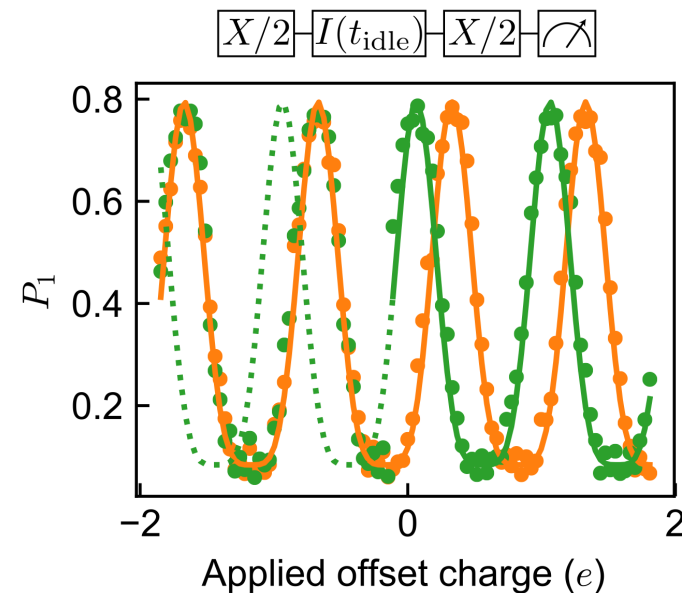
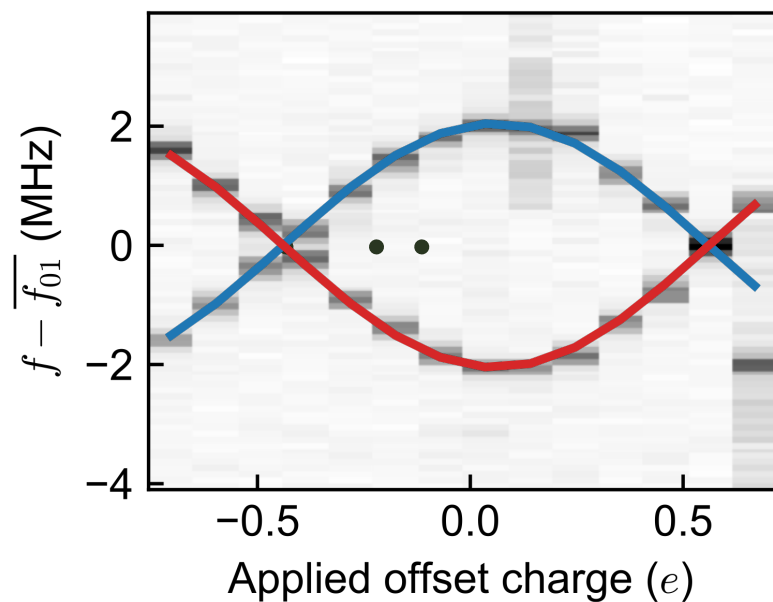
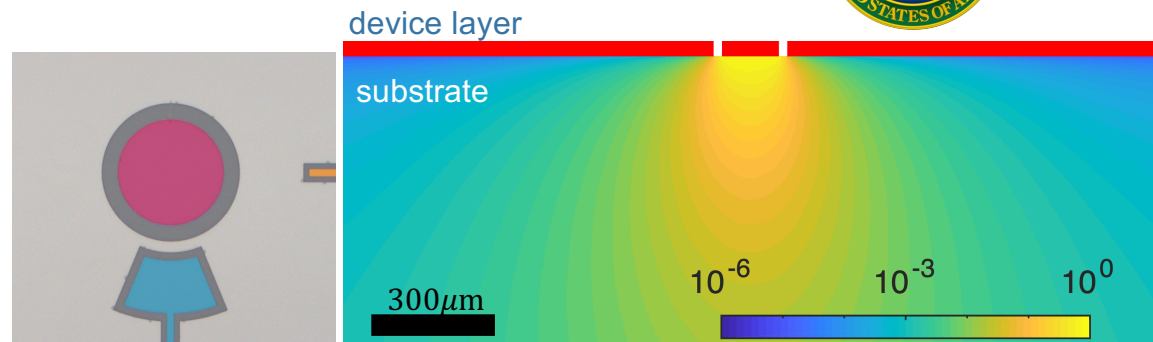
# Correlated errors in SC multiqubit circuits

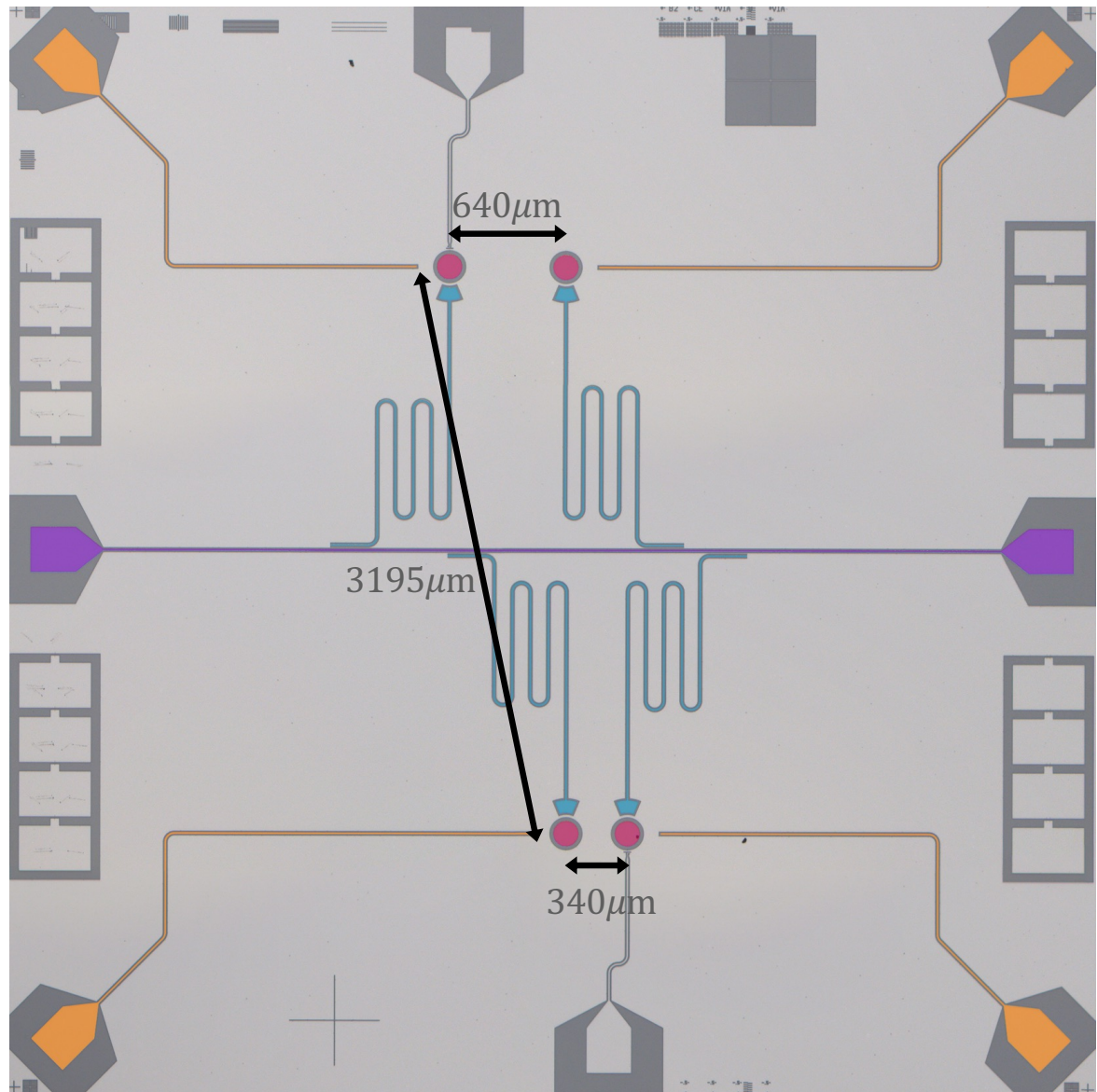
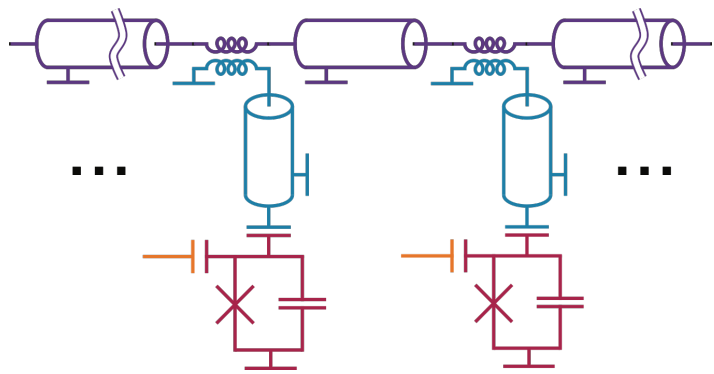
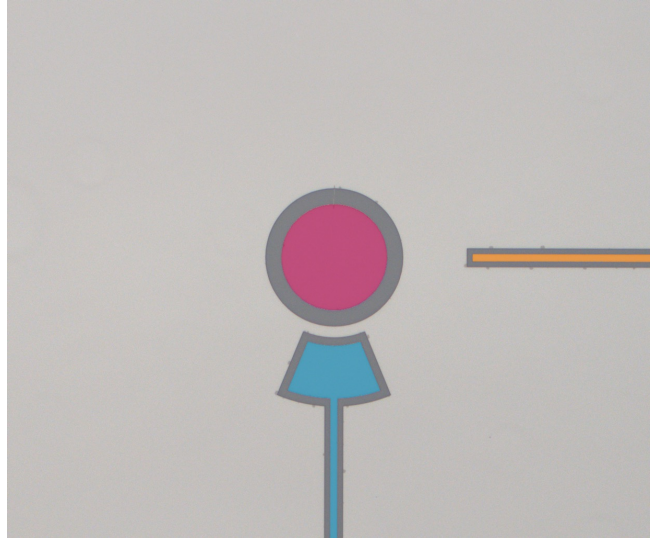
(prior DOE project)

Wilen *et al.*, Nature **594**, 7863 (2021)



- Qubit as electrometer
- $E_J/E_C \sim 25$
- Ramsey-based charge tomography

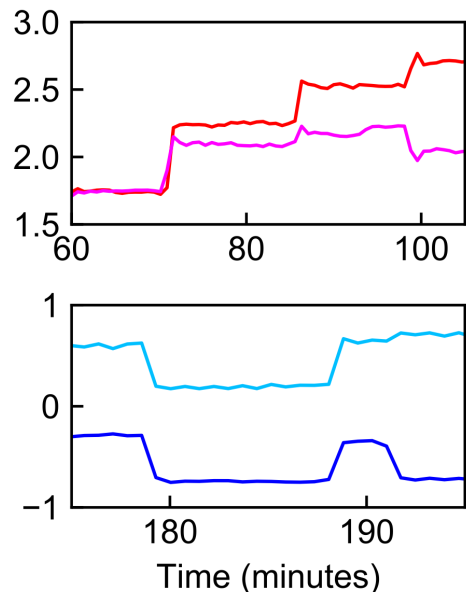
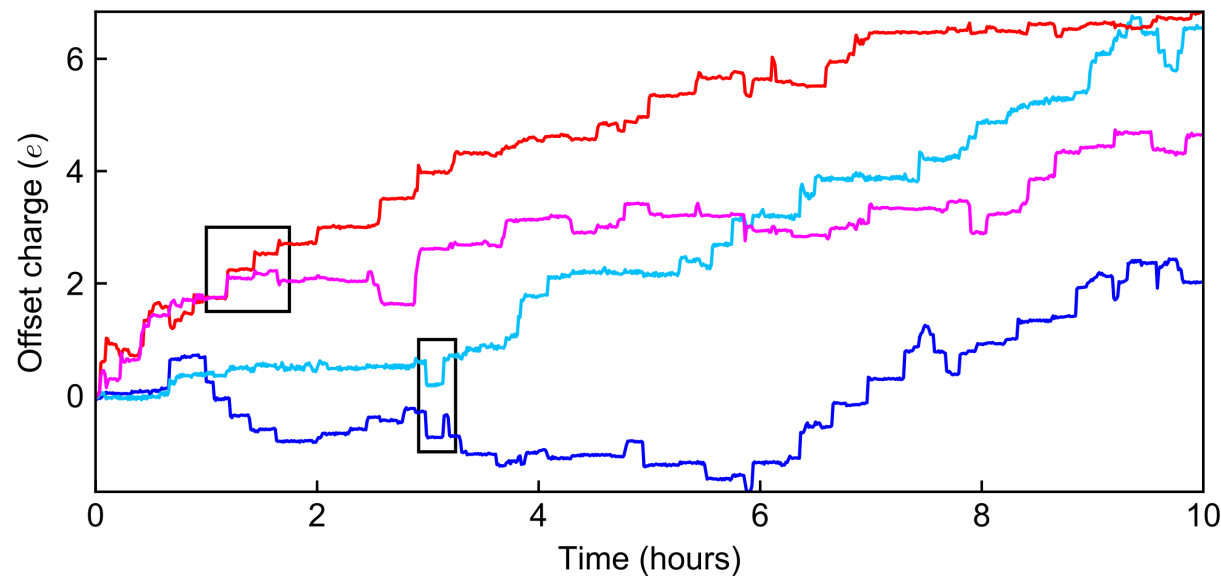
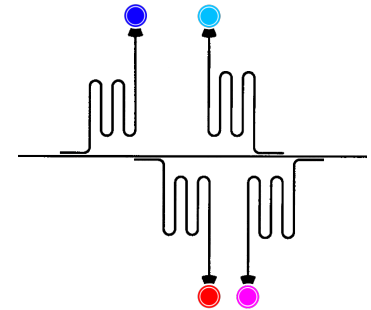


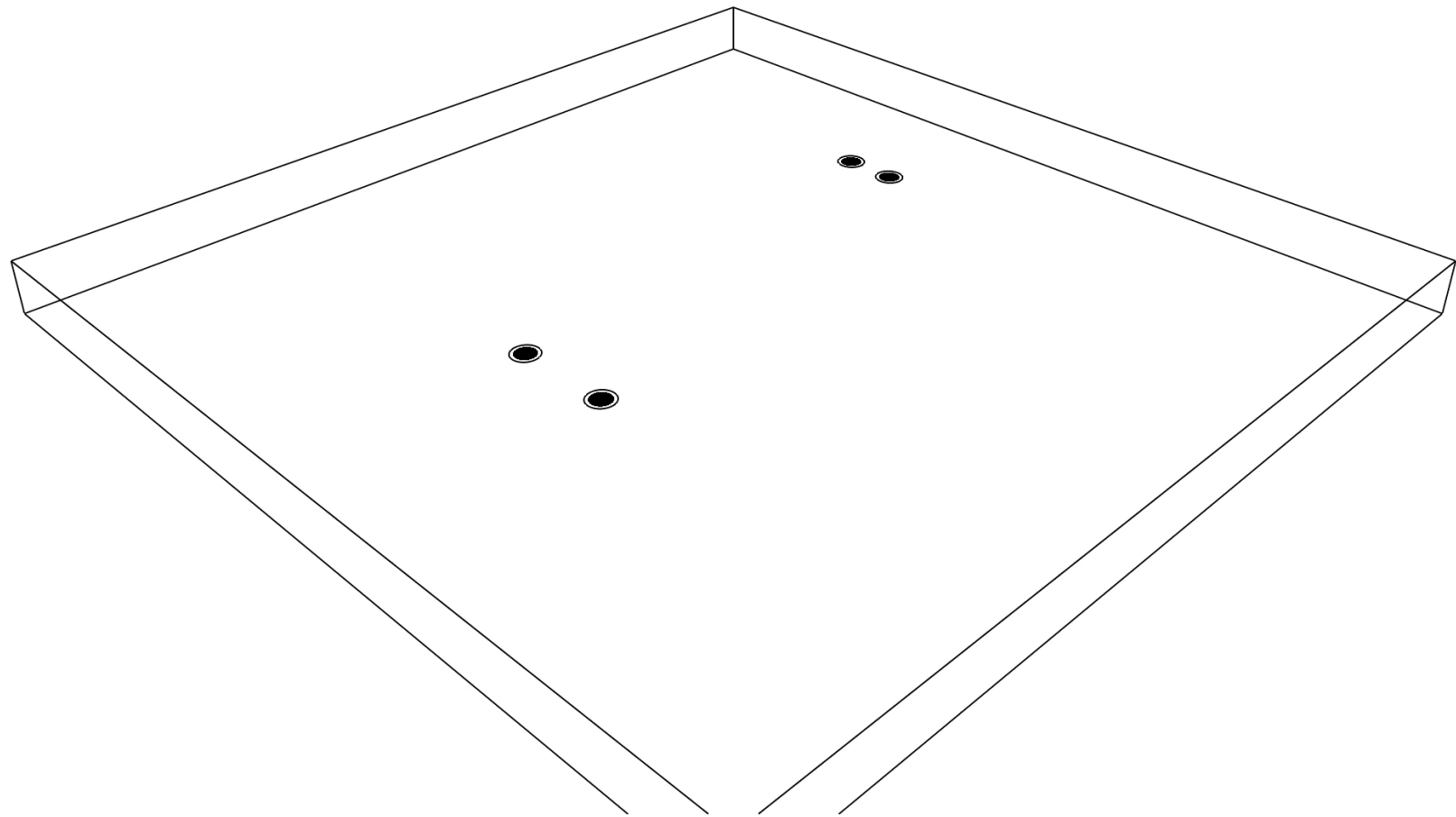


# Correlated charge fluctuations

- Large discrete jumps
- Correlated jumps in neighboring qubits

Riste et al., Nat. Comm. **4**, 1913 (2013).  
Serniak et al., PRL **121**, 157701 (2018).  
Christensen et al., PRB **100**, 140503 (R)(2019).



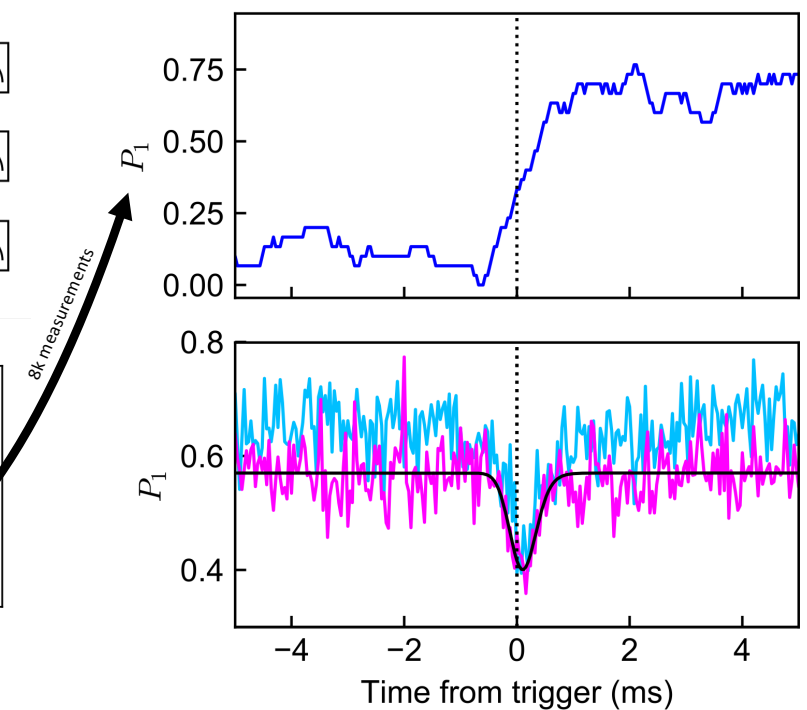
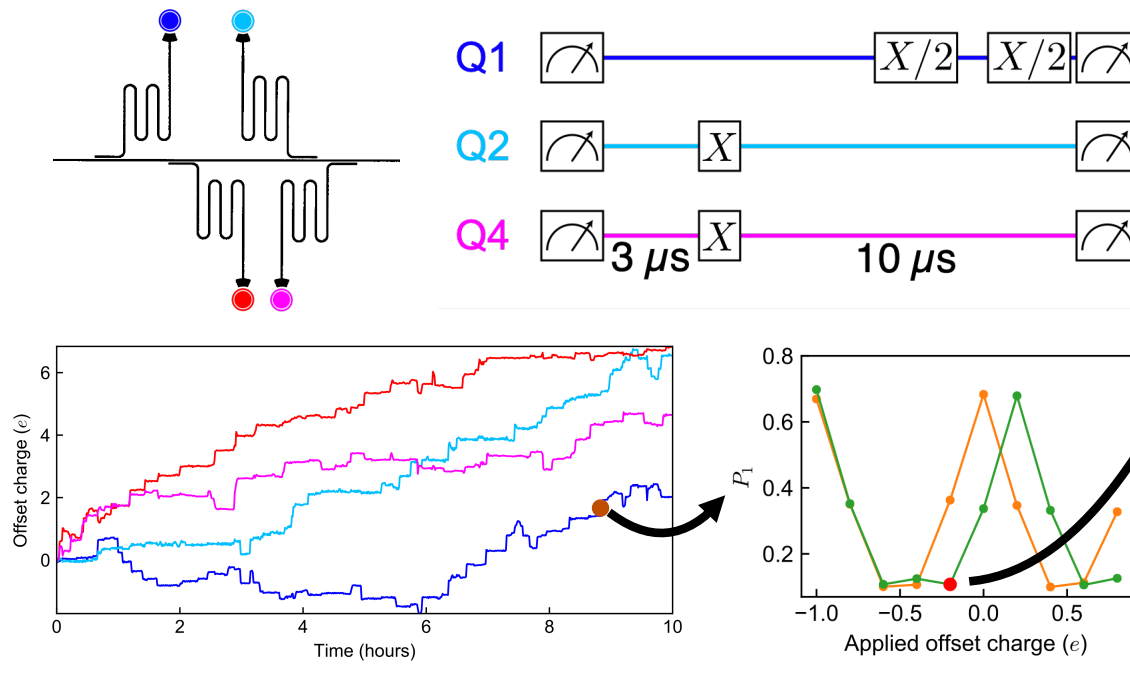


# Correlated relaxation errors

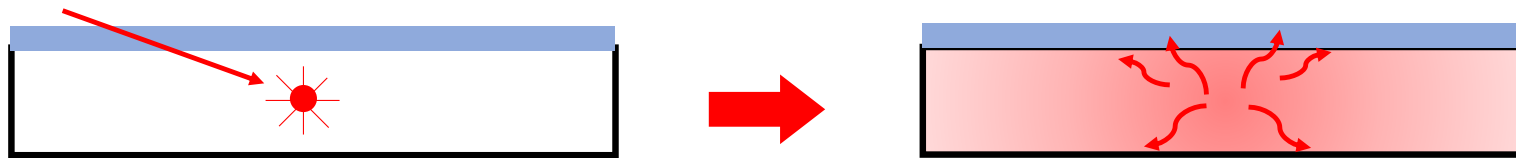
- Use jumps in Ramsey measurement as trigger
- Seen across distances > 3 mm

recovery timescale

$$\tau = 130 \pm 40 \mu\text{s}$$



# Phonon-mediated quasiparticle poisoning

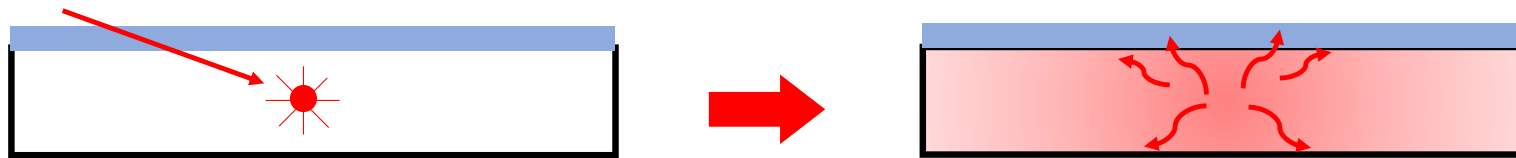


- 95% of deposited energy coupled to phonon reservoir  
[CDMS: e.g., Shutt et al., PRL 69, 3531 (1992)]
  - Weak acoustic coupling to environment
  - Few relaxation channels below SC gap edge
  - Correlated pair-breaking across the chip

Possible mitigation strategies:

- Superconducting gap engineering
- Backside normal metallization
- Micromachining to suppress phonon transport
- Shielding to suppress absorption of HE particles

# Phonon-mediated quasiparticle poisoning



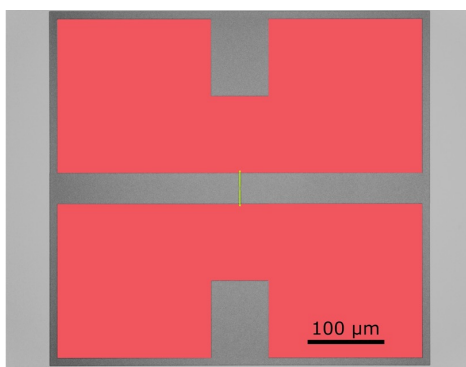
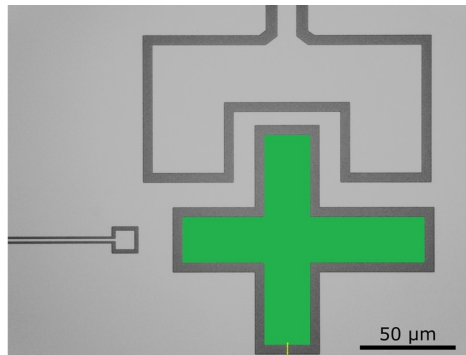
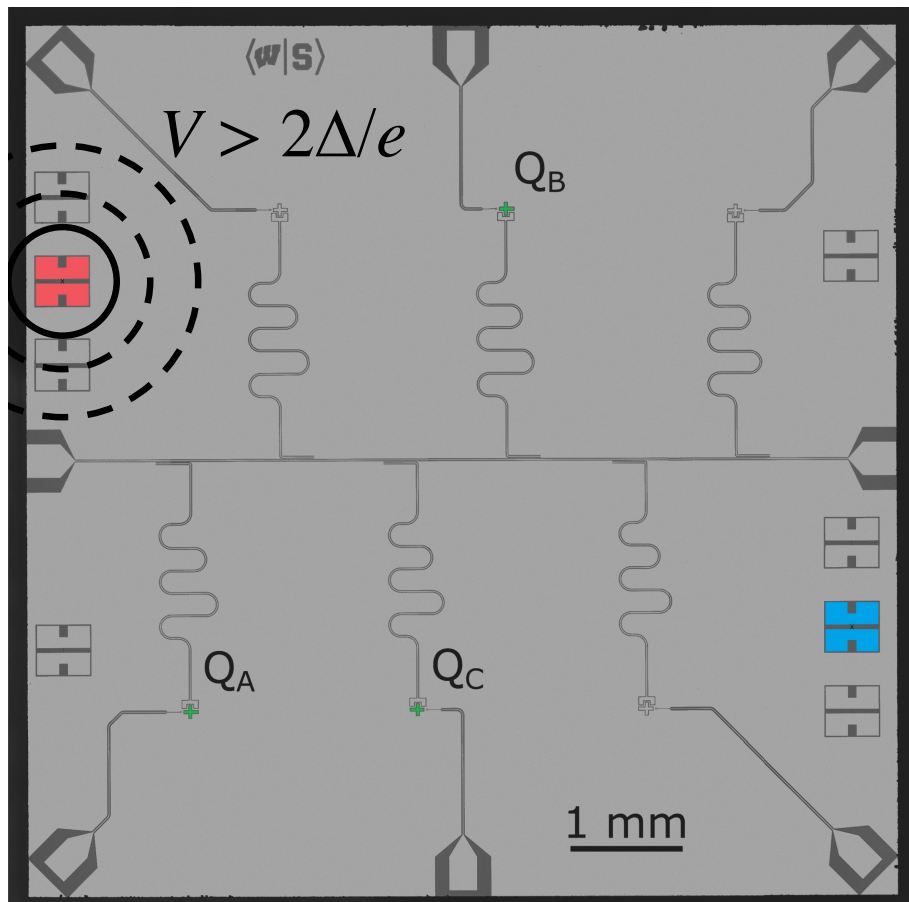
- 95% of deposited energy coupled to phonon reservoir  
(CDMS: e.g., Shutt et al., PRL 69, 3531 (1992))
  - Weak acoustic coupling to environment
  - Few relaxation channels below SC gap edge
  - Correlated pair-breaking across the chip

Possible mitigation strategies:

- Superconducting gap engineering
- Backside normal metallization
- Micromachining to suppress phonon transport
- Shielding to suppress absorption of HE particles

# Controlled study of phonon-mediated QP poisoning

(With B. Plourde group, Syracuse U.)

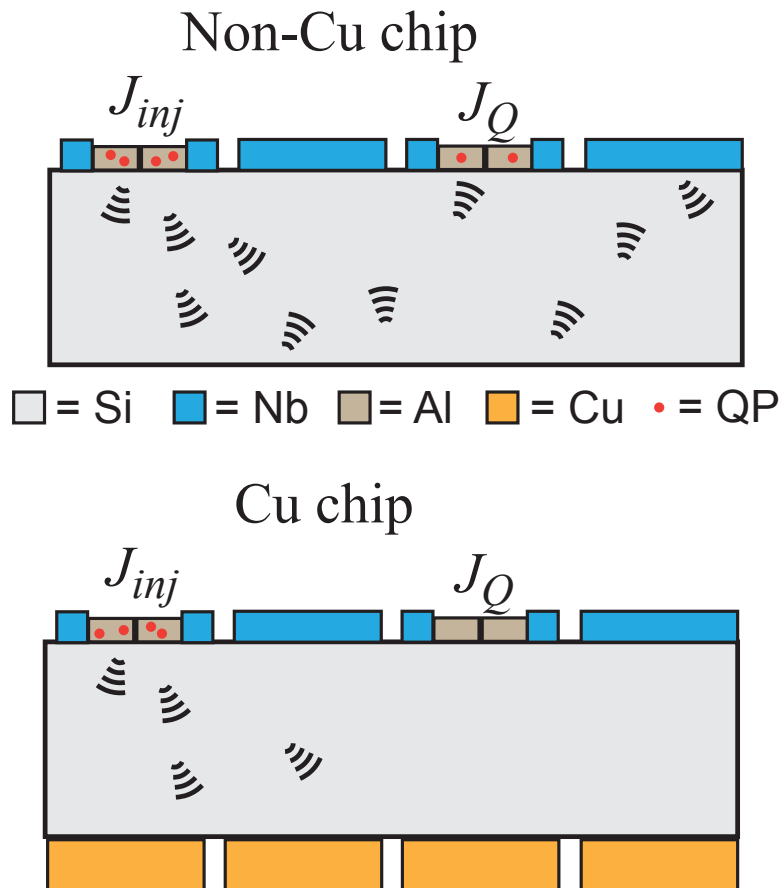


- Nb groundplane, 70 nm
- Al/AlOx/Al JJ, 360 x 150 nm<sup>2</sup>
- Cavities: 5.9 - 6.5 GHz
- Qubits: 4.9 - 5.1 GHz
- $E_J/E_c \sim 30$

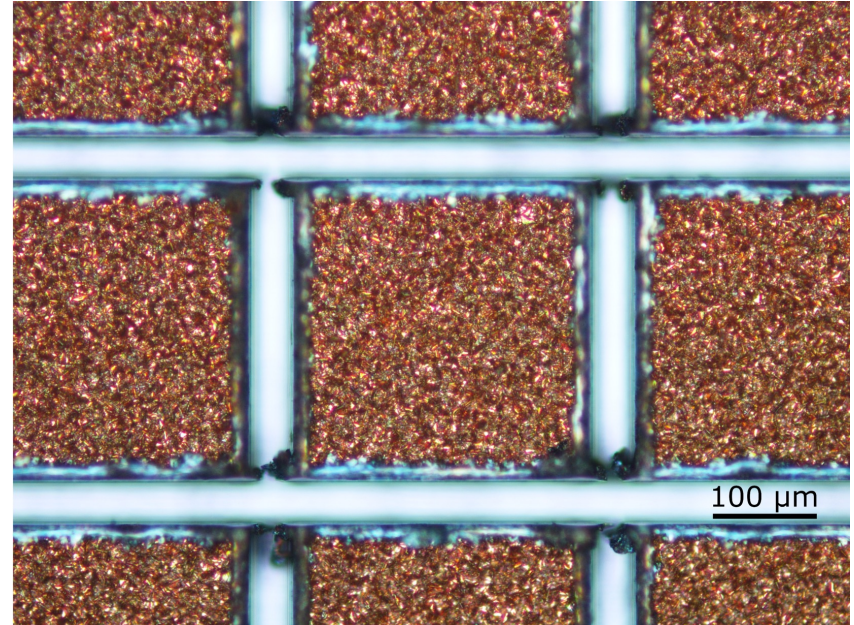
- Injector JJs: 1 μm x 150 nm
- $I_c \sim 100$  nA
- No galvanic connection to groundplane

# Controlled study of phonon-mediated QP poisoning

(With B. Plourde group, Syracuse U.)



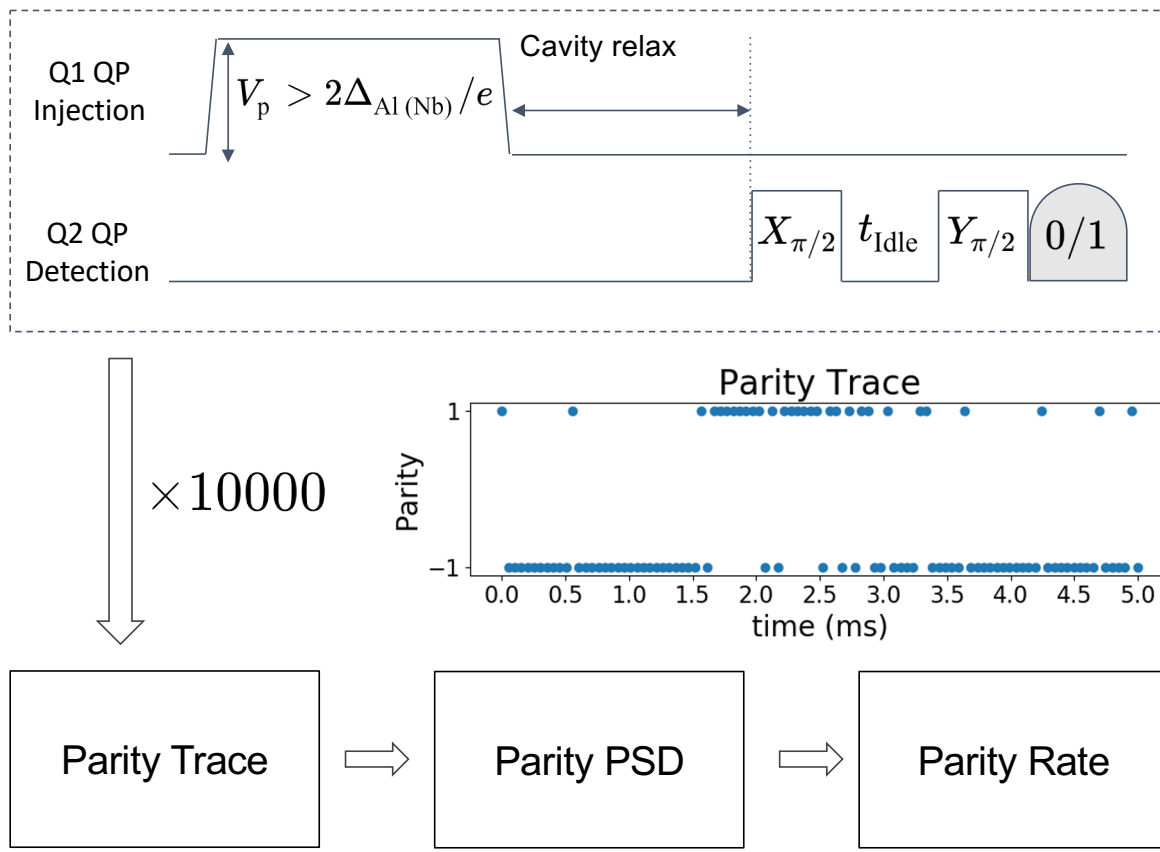
Electroplated Cu  
10  $\mu\text{m}$  thick  
RRR  $\sim 42$



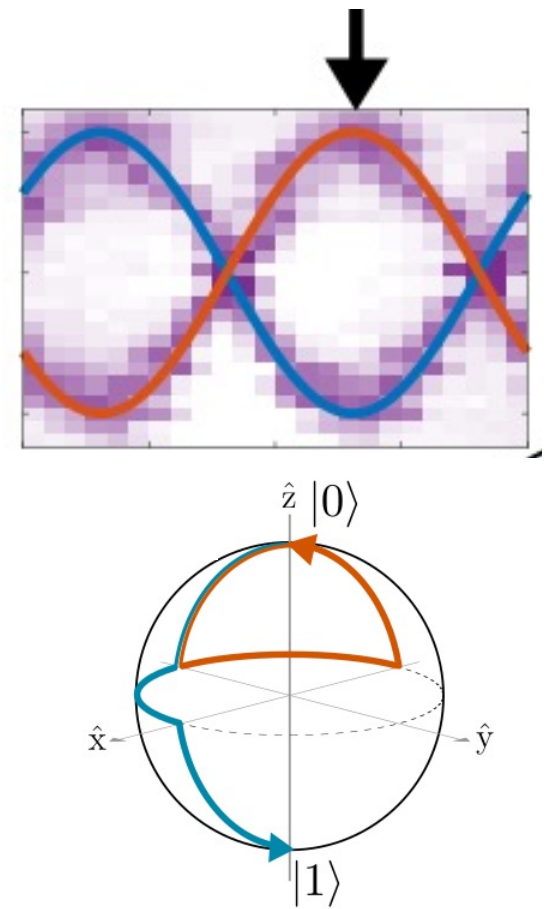
# Direct measurement of QP poisoning via charge parity

Riste et al., Nat. Comm. **4**, 1913 (2013)

Serniak et al., PRL **121**, 157701 (2018)

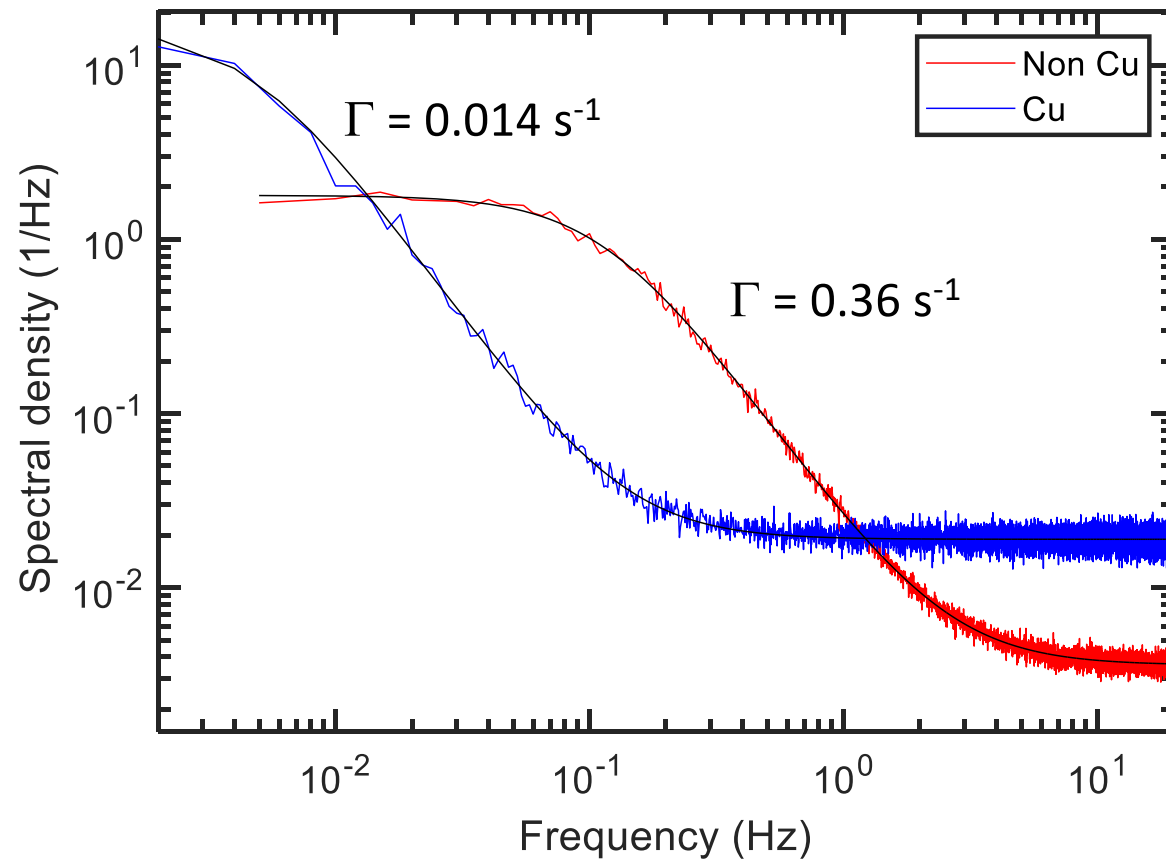


bias at maximum charge dispersion

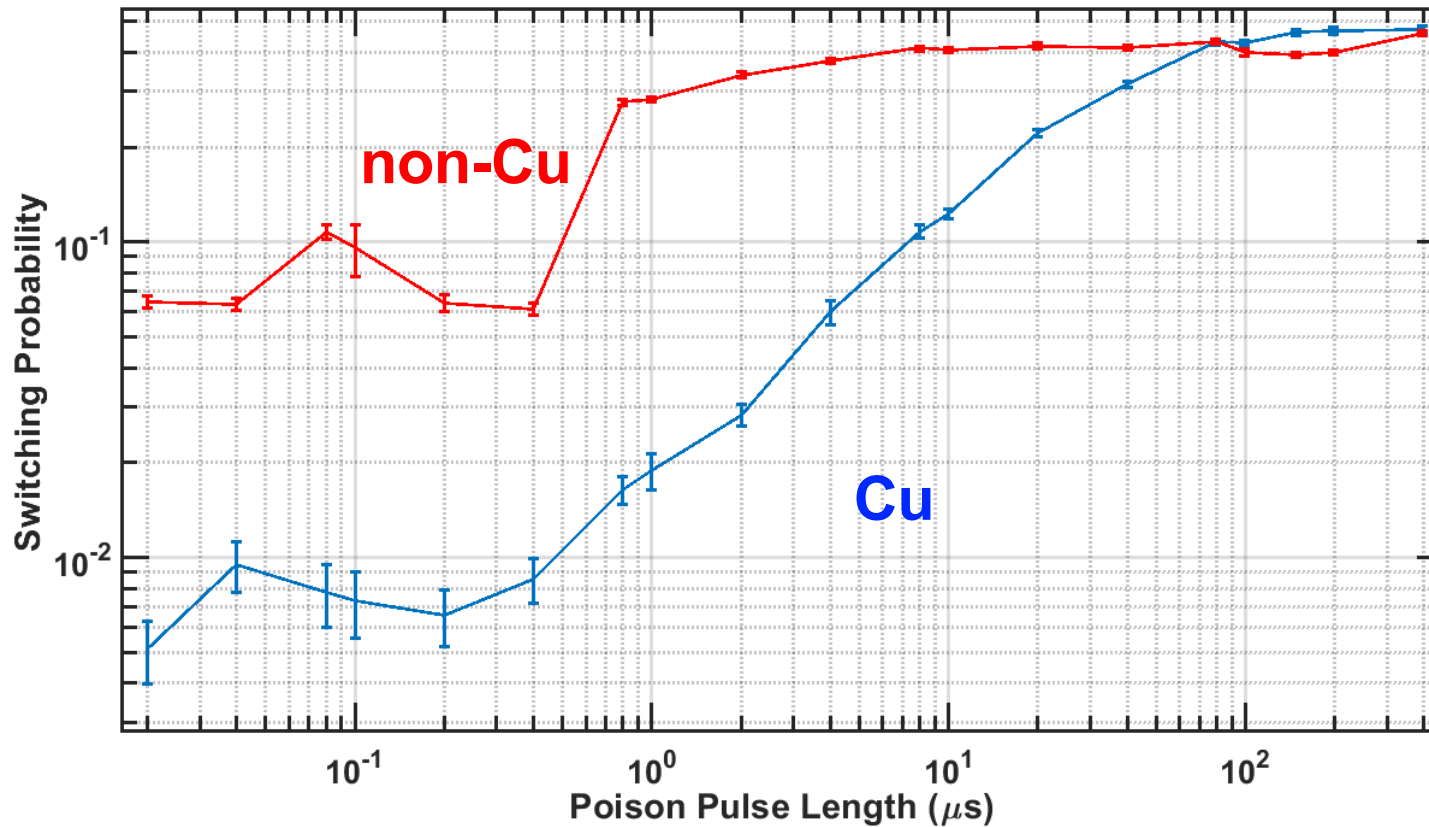


# Direct measurement of QP poisoning via charge parity

Baseline:  
no QP injection



## Simultaneous parity monitoring with phonon injection



## No injection: suppression of correlated error from impact events

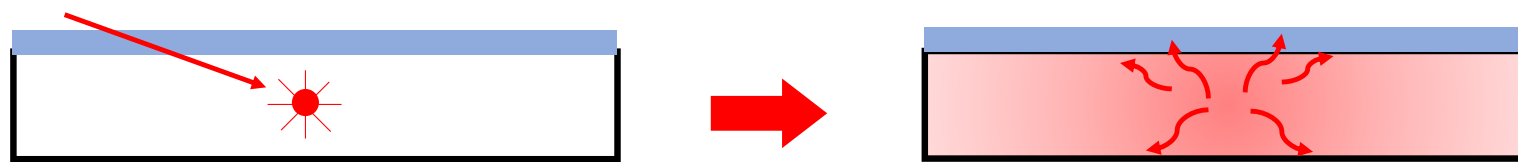
Device	Observed parity switching rates ( $\text{s}^{-1}$ )						
	$Q_A$	$Q_B$	$Q_C$	$Q_A \wedge Q_B$	$Q_B \wedge Q_C$	$Q_A \wedge Q_C$	$Q_A \wedge Q_B \wedge Q_C$
Non-Cu	0.309(3)	0.313(4)	0.301(3)	0.073(2)	0.068(2)	0.064(2)	0.0134(9)
Cu	0.0250(4)	0.0344(5)	0.0545(6)	0.0014(1)	0.00357(2)	0.0062(3)	0.00012(6)
spacing	-	-	-	5.3 mm	4.5 mm	2.0 mm	-

Expected random coincident parity switching rates ( $\text{s}^{-1}$ )				
Device	$Q_A \wedge Q_B$	$Q_B \wedge Q_C$	$Q_A \wedge Q_C$	$Q_A \wedge Q_B \wedge Q_C$
Non-Cu	0.039(5)	0.038(5)	0.037(5)	0.005(6)
Cu	0.0003(6)	0.0007(8)	0.0005(7)	0.000007(852)

$$(r_A^{\text{obs}} \Delta t)(r_B^{\text{obs}} \Delta t)/\Delta t \quad (r_A^{\text{obs}} \Delta t)(r_B^{\text{obs}} \Delta t)(r_C^{\text{obs}} \Delta t)/\Delta t$$

Device	Extracted poisoning rates ( $\text{s}^{-1}$ )						
	$Q_A$	$Q_B$	$Q_C$	$Q_A \wedge Q_B$	$Q_B \wedge Q_C$	$Q_A \wedge Q_C$	$Q_A \wedge Q_B \wedge Q_C$
Non-Cu	0.16(2)	0.16(2)	0.16(1)	0.21(1)	0.19(1)	0.18(1)	0.070(6)
Cu	0.021(2)	0.051(2)	0.072(2)	0.0049(7)	0.013(1)	0.024(1)	0.0002(5)
spacing	-	-	-	5.3 mm	4.5 mm	2.0 mm	-

# Are particle impacts the source of nonequilibrium QPs?



Density of QPs in SC devices far exceeds thermal equilibrium value expected from theory (typ.  $1 \mu\text{m}^{-3}$ )

- Poisoning of charge-sensitive devices [cf. Aumentado et al., PRL **92**, 066802 (2004)].
- Enhanced qubit relaxation [Corcoles et al., APL **99**, 181906 (2011)].
- Qubit initialization errors of order 1-3%

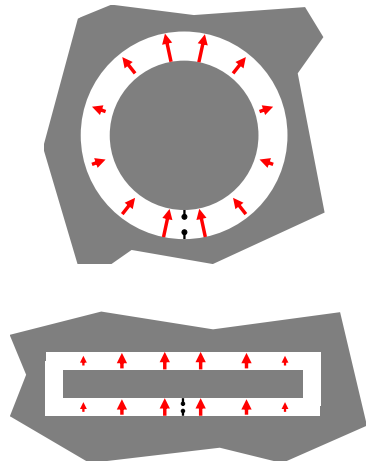
MIT/LL group: model for QP poisoning from gamma impacts [Vepsalainen et al., Nature **584**, 551 (2020)]

However, event rate too low and escape rate of athermal phonons too high to account for measured QP densities in most devices

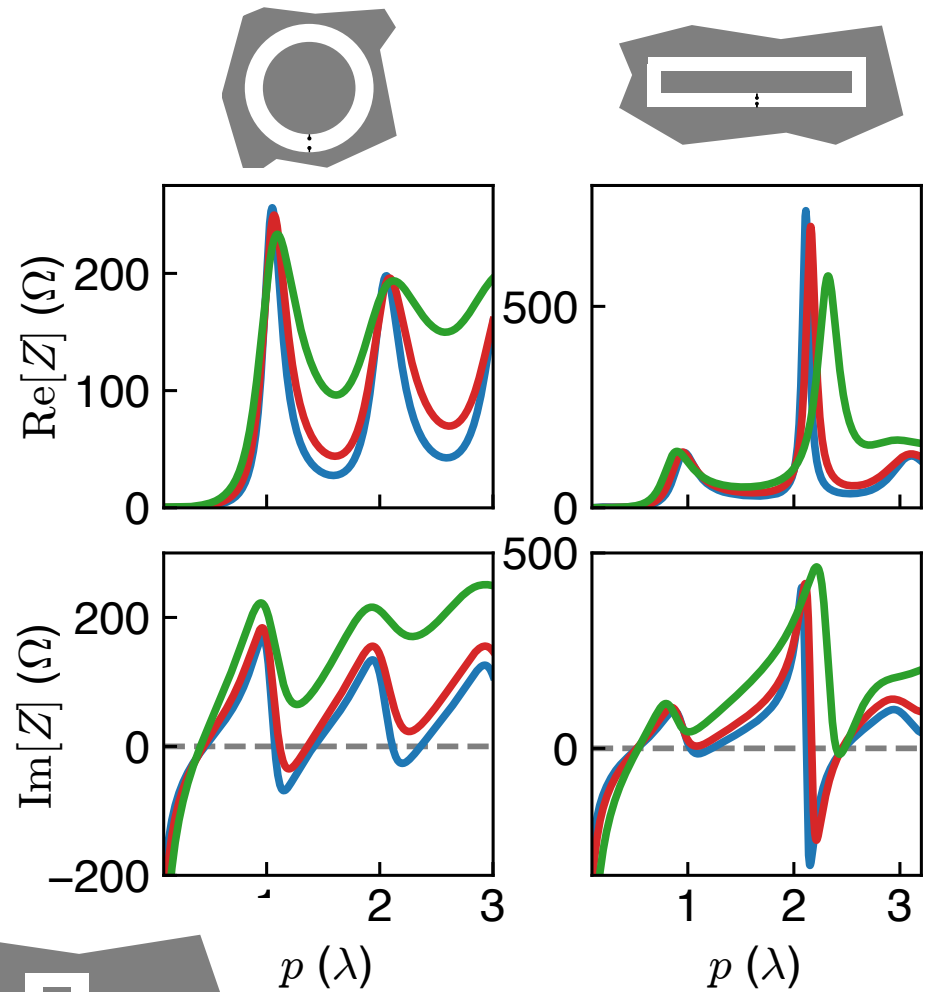
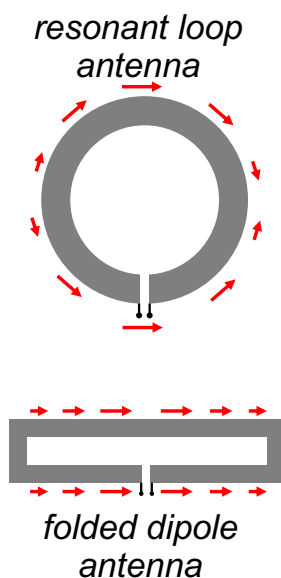
# Antenna modes of the transmon qubit

Rafferty et al., arXiv:2103.06803 (2021)

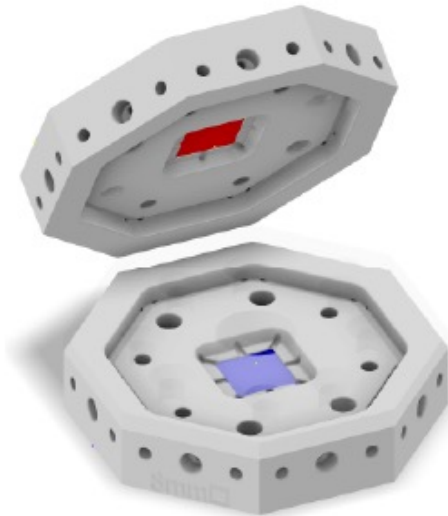
Typ. SC  
qubit structures



Wire antenna  
duals

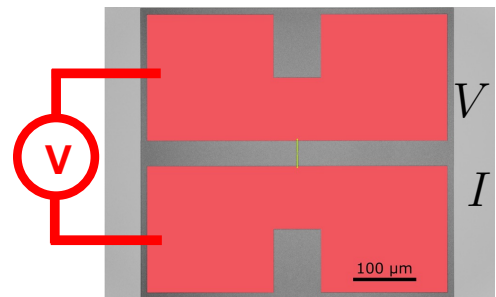
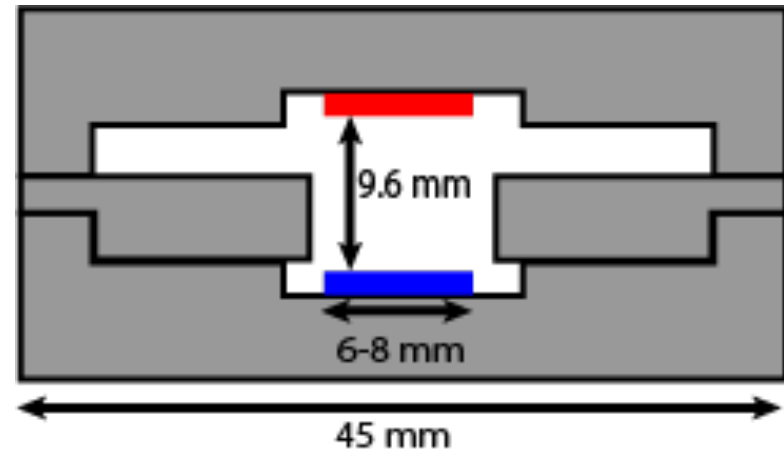


# Validation of antenna model



transmitter

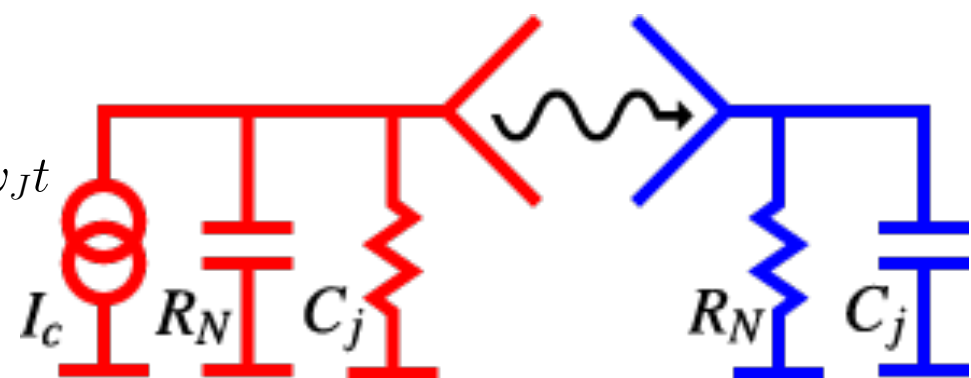
receiver



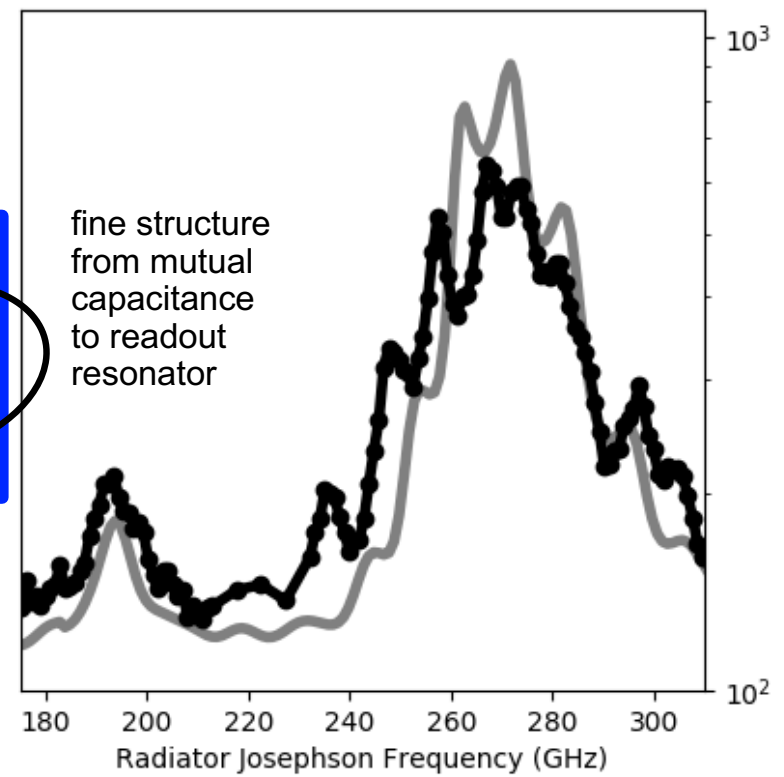
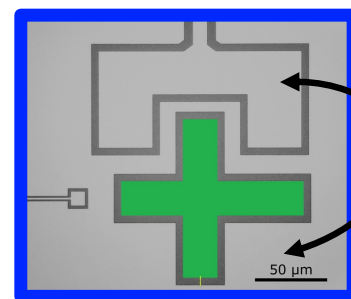
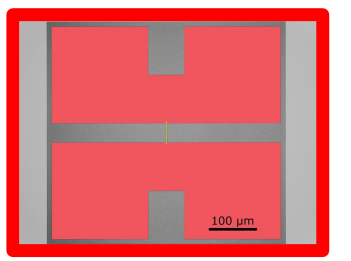
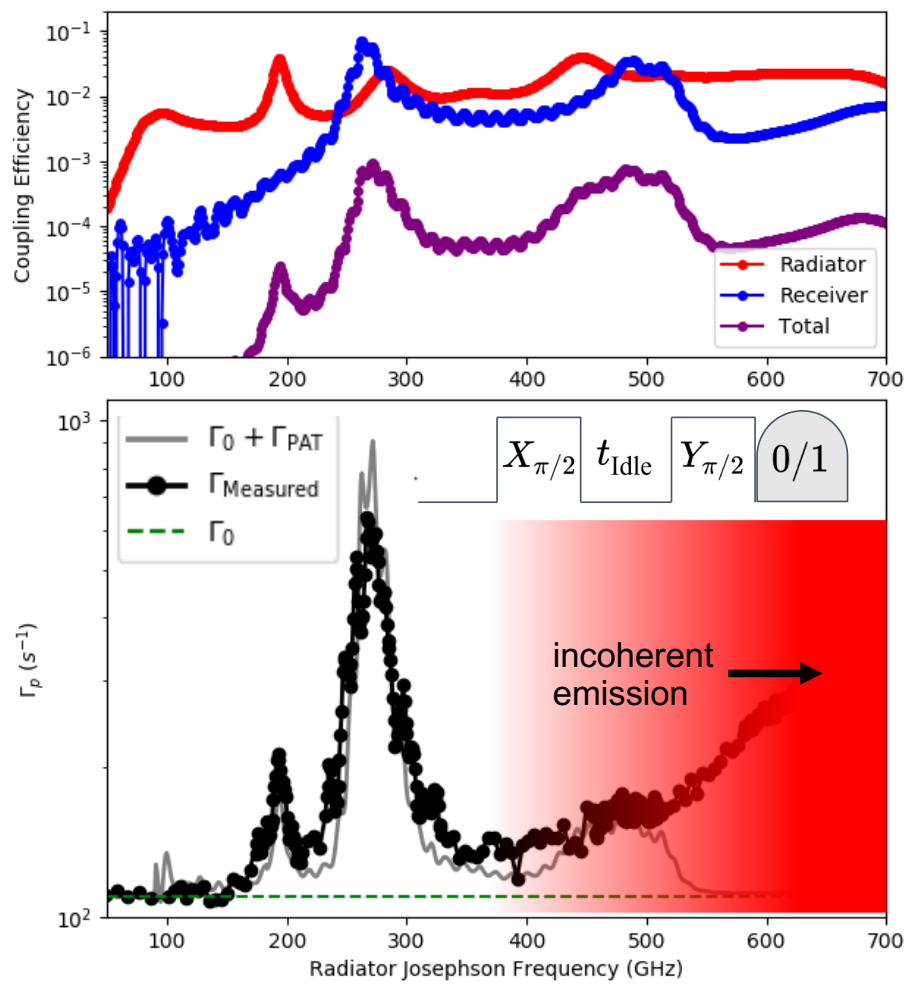
$$V = \frac{\Phi_0}{2\pi} \dot{\delta}$$
$$I = I_c \sin \delta$$



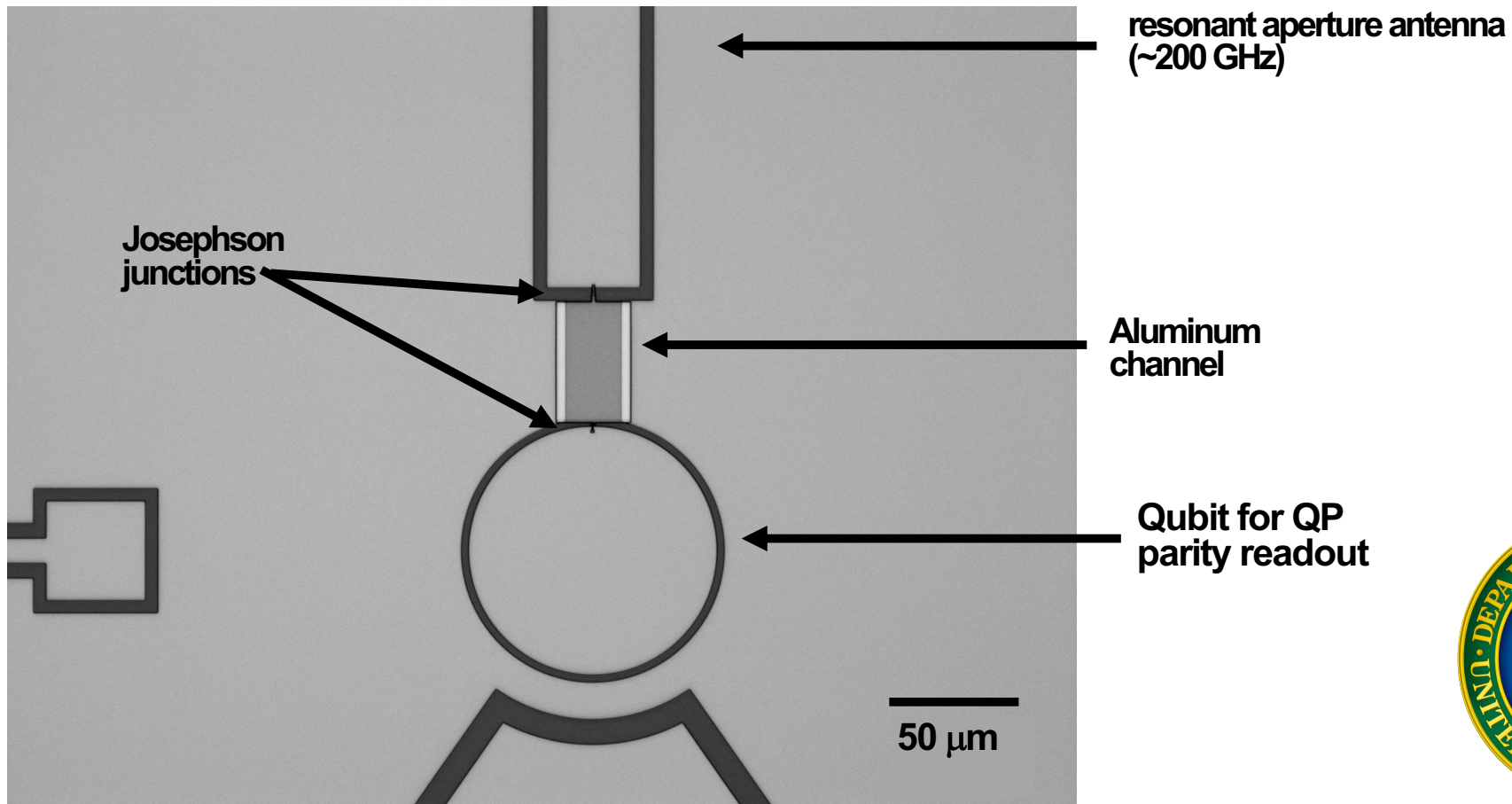
$$I = I_c \sin \omega_J t$$
$$f_J = V/\Phi_0$$



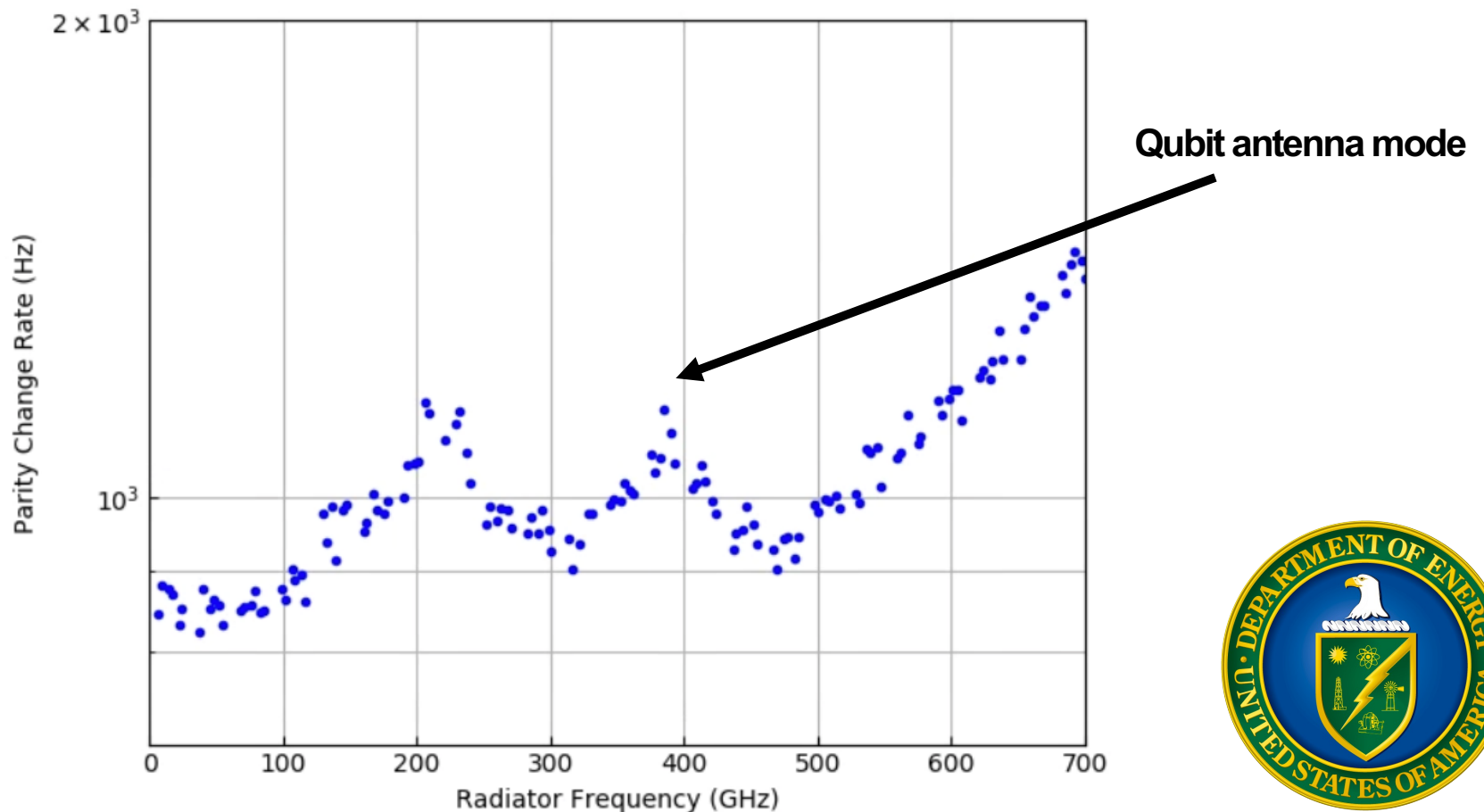
# Validation of antenna model



# Modular detector for axion search



# Modular detector for axion search



# Acknowledgments

Aaron Chou, FNAL (DOE QuantISED Program Lead)

UW-Madison:

D. Harrison (PD)  
C. H. Liu (GS)  
S. Patel (GS)  
O. Rafferty (UG)

S. Abdullah (GS)  
F. Schlenker (Res. Sci.)  
C. D. Wilen (GS)

# Conclusion

- Particle impacts give rise to damaging correlated errors on length scales greater than 3 mm: relaxation errors must be mitigated
- Phonon downconversion yields dramatic suppression of correlated parity jumps
- Detailed understanding of photon-assisted QP poisoning
- New class of modular detectors for dark-matter searches

